sociedade & natureza

DOI: 10.14393/SN-v34-2022-64381
Received: January 27, 2022 | Accepted: April 13, 2022 | Published: June 20, 2022

Papers

Sedimentology and volumetric reconstitution of mud flow deposits in an alluvial plain: study in the Jacareí River basin, Paraná

Otacílio Lopes de Souza da Paz[1]
Eduardo Vedor de Paula[2]

Keywords:
River geomorphology
Sediments
Landscape transformation

Abstract
Extreme mud and debris flows can bury alluvial plains. In current literature, there exists a significant knowledge gap regarding this process, since information about the sedimentological characteristics and estimates of the volumes of these deposits, are still scarce. Such knowledge is important for understanding the role of these events in the morphogenesis of the alluvial plains of the highland mountain margins. The study area located in the Jacareí River basin (coast of the State of Paraná, Brazil) was recently buried by mud slides in March 2011, therefore, our objective is to analyze the sedimentology and estimate the volume of instantaneous deposits formed by the aforementioned gravitational processes. The deposits were mapped based on a geospatial database. Afterwards, samples were collected for laboratory analysis. To estimate the volume, field samples were collected, measuring the thickness of the deposits, which were then interpolated in a GIS environment. Pelitic (9%), psephytic (4%) and psammitic (87%) deposits were identified. The psammitic deposits showed two distinct behaviors as a function of the flow and burial dynamics of the alluvial plain. The total volume of the deposit was estimated at 1,7 million tons of sediment. The results demonstrate the magnitude of the 2011 event, since in a period of less than 24 hours the Jacareí river basin moved more than 8.5 times the annual production of sediments from the hydrographic units that drain into the Estuarine Complex of Paranaguá.

[1] Universidade Federal do Paraná – UFPR, Curitiba, PR, Brazil. otacilio.paz@gmail.com
[2] Universidade Federal do Paraná – UFPR, Curitiba, PR, Brazil. edugeo@ufpr.br

INTRODUCTION

Mud and debris flows are fast gravitational flows composed of a concentrated mixture of sediment, organic matter, and water (HUNGR et al, 2014). These events are commonly triggered by landslides associated with intense precipitation (COSTA, 1984; HUNGR, 2005). It is an important geomorphological agent in mountain landscapes, closely related to the process of relief denudation.

The high density of these mass flows allows the transportation of clasts ranging from sand fractions to boulders (LI et al., 2015; WANG et al., 2018; YANG et al., 2019). The resulting sedimentary deposits are commonly found in intramontane riverbeds and river mouths, forming alluvial fans. (COSTA, 1984; HUNGR, 2005). Due to their high speed, energy and volume, these processes have a high destructive potential, posing risks to structures and populations. (FROUDE; PETLEY, 2018).

The Serra do Mar is located along the southern and southeastern coastal region of Brazil, it consists of a system of escarpments and mountains with remarkable lithological and structural complexity, with steep slopes and high average precipitation over prolonged periods, especially in the summer months (VIEIRA; GRAMANI, 2015). These characteristics makes the landscape susceptible to the occurrence of mud and debris flows (KOBIYAMA et al., 2015; VIEIRA; GRAMANI, 2015; ROSS; FIERZ, 2018).

Teixeira and Satyamurty (2011), when analyzing precipitation data in the southern and southeastern regions of Brazil, identified an increase in the frequency of intense and extreme rainfall events between 1960-2004, with a statistically significant trend in the southern region. The authors point out that this could already be a result of climate change in the region, however, longer time series are required to corroborate this hypothesis. Recent studies have correlated the increase in the number of intense and extreme rainfall events with the increase in the frequency and magnitude of gravitational processes (mud and debris slides and flows), in Brazil (ÁVILA et al., 2016; AVILA-DIAZ et al., 2020) and around the globe (BORGA et al., 2014; KUMARI et al, 2021).

In events of greater magnitude, mud and debris flows can reach extensive areas in the floodplains, generating floods and forming "instant deposits", which are similar to "flash flood deposits", and are understood as sedimentary deposits formed in a short period, by floods with high sedimentary load, induced by mud and debris flows (ORTEGA; GARZÓN HEYDT, 2009; PAREDES et al., 2021).

An example of this process is found in part of the Jacareí River plain (coast of the State of Paraná), which was strongly affected by gravitational processes in March 2011, forming deposits in the intramontane channels, in the river mouths and in the alluvial plain (PINTO et al; 2012; SILVEIRA et al., 2013). This spatial and temporal scope makes the Jacareí River plain an ideal study area, as it is still possible to identify in the field the impacts of the mud flow event on the sedimentary records of the plain, which are well preserved.

The event in the Jacareí River basin in 2011, motivated increased research efforts focused on the characterization of the processes (PINTO et al. 2012; PICANÇO; NUNES, 2013) and mapping of the susceptibility to gravitational processes (SILVEIRA et al., 2014; FACURI; PICANÇO, 2021). However, no studies were carried out on the generated deposits in the floodplain, which was completely buried by the event.

In Brazil, only a small number of studies have been dedicated to the description of sedimentology and estimates of volumes of newly generated deposits. (BIGARELLA, 2003; GRAMANI, 2018). Existing descriptions are mostly based on intramontane deposits located in and around river channels, directly affected by the flows. Questions about the sedimentology and estimates of the volumes of these deposits from the mud flows in alluvial plains remain unknown.

Both the sedimentological analysis and the estimation of the deposited volume are important to understand the role of these events in the morphogenesis of the alluvial plains of the highland mountain margin. Therefore, considering the identified knowledge gap and the characteristics of the alluvial plain of the Jacareí River as the study area, the objective is to carry out a sedimentological analysis and estimate the volume of flash flood deposits generated after the mass flow events that occurred in March 2011.

MATERIALS AND METHODS

Study area

The Jacareí River plain is located between the municipalities of Paranaguá and Morretes, on the Paraná coast. The study area focuses on one stretch of the floodplain, limited between the 30-meter elevation and the BR 277 highway embankment, which was the portion most affected by the March 2011 event (Figure 1). Downstream of the landfill, the Jacareí River plain is composed of a mosaic of river, marine, estuarine and swamp deposits (ANGULO, 2004; MINEROPAR, 2006). The Jacareí River Basin (JRB) encompasses 41.28 km², while our study area is 2.86 km².

Figure 1 - Location of the Jacareí river floodplain affected by the 2011 event.

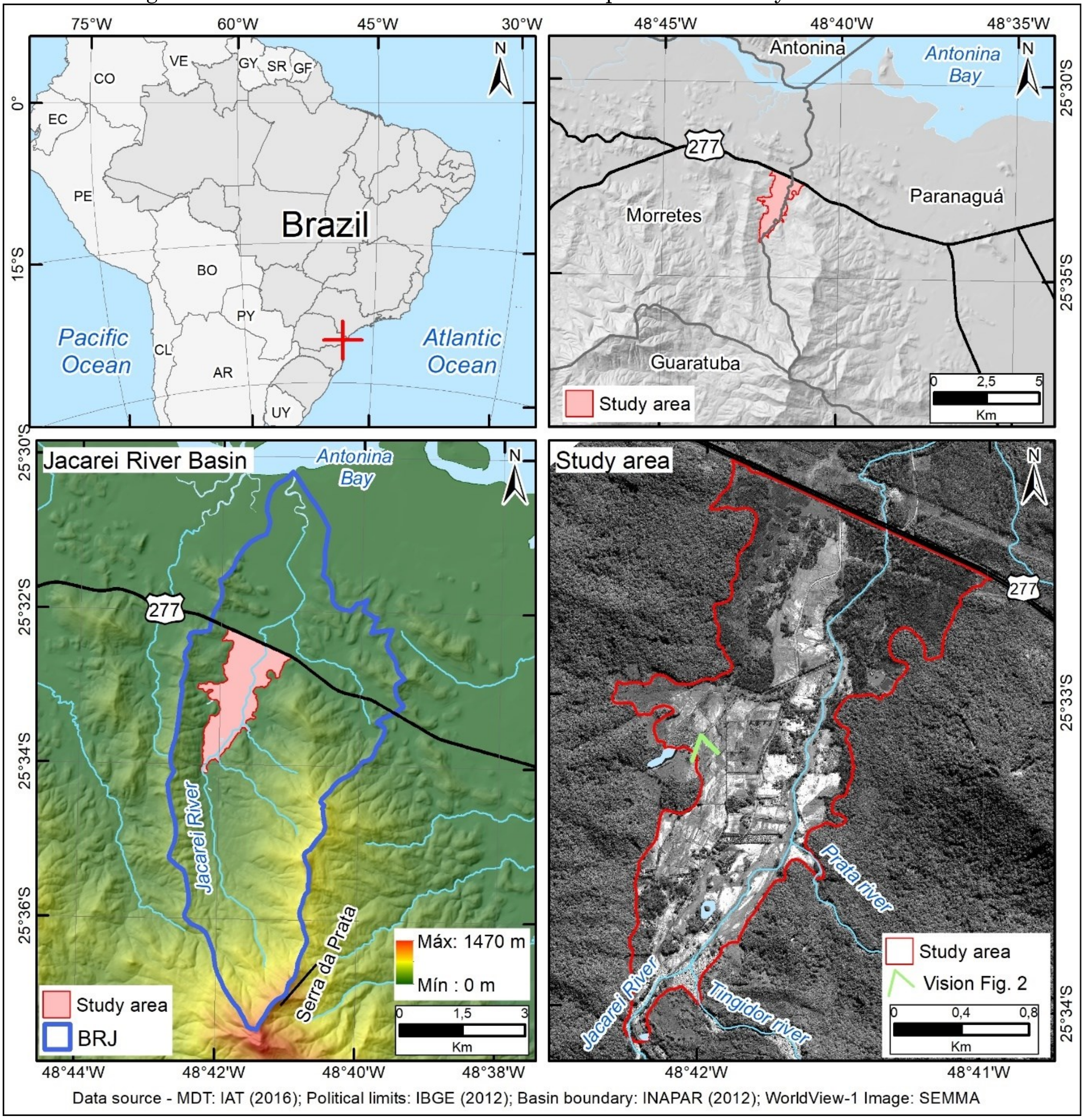

Source: The authors (2022).

In the study area, the Tingidor and Prata rivers are the only perennial-flow tributaries to the Jacareí River, both on its right riverbank. The hydrographical dividers from east to south are located in the Serra da Prata, a core of the Serras Altas which is supported by granite-gneiss-migmatitic rocks related to the Cachoeira Complex. (MINEROPAR, 2006), presenting altitudes between 800 and 1421 meters. The western hydrographical dividers present altitudes between 200 and 433 meters and are composed of undifferentiated metamorphic rocks of the Rio das Cobras Formation (MINEROPAR, 2011).

In the study area, the Jacareí River has a length of 3.65 km and a straight pattern (1,14 in the sinuosity index in 2020) and a general northeast-north direction, with its mouth in the Antonina Bay, head of the Estuarine Complex of Paranaguá. The JRB is mostly composed of vegetation in the arboreal stratum, concentrated in the higher portions of the terrain (from 50 meters of altitude). Human activities predominate in the plain and in parts of the lower thirds of the slopes, with agricultural activities (cassava, chives and ginger), livestock (cattle, buffalo and, before the 2011 event, goat farming), forestry (pine and eucalyptus) and mineral extraction (sand from the Jacareí river and its banks).

The studied event occurred on 11/03/2011 and profoundly transformed the sedimentary records of the Jacareí River floodplain (Figure 2). After an accumulated rainfall of 236,8 mm in 24 hours (higher than the expected precipitation for the entire month of March), several landslides occurred in the upper third of the slopes of the Serra da Prata. (SILVEIRA et al., 2014; ZAPATA et al., 2016). The alluvial plain, between the foothills of the slopes (30 meters in altitude) to the embankment of the BR 277 highway, was buried, while the Serra da Prata was marked by dozens of scars (Figure 2).

Figure 2 – JRB landscape after the gravitational processes of 11/03/2011. Note the scars in the Serra da Prata and the intense contribution of sediments in the alluvial plain.

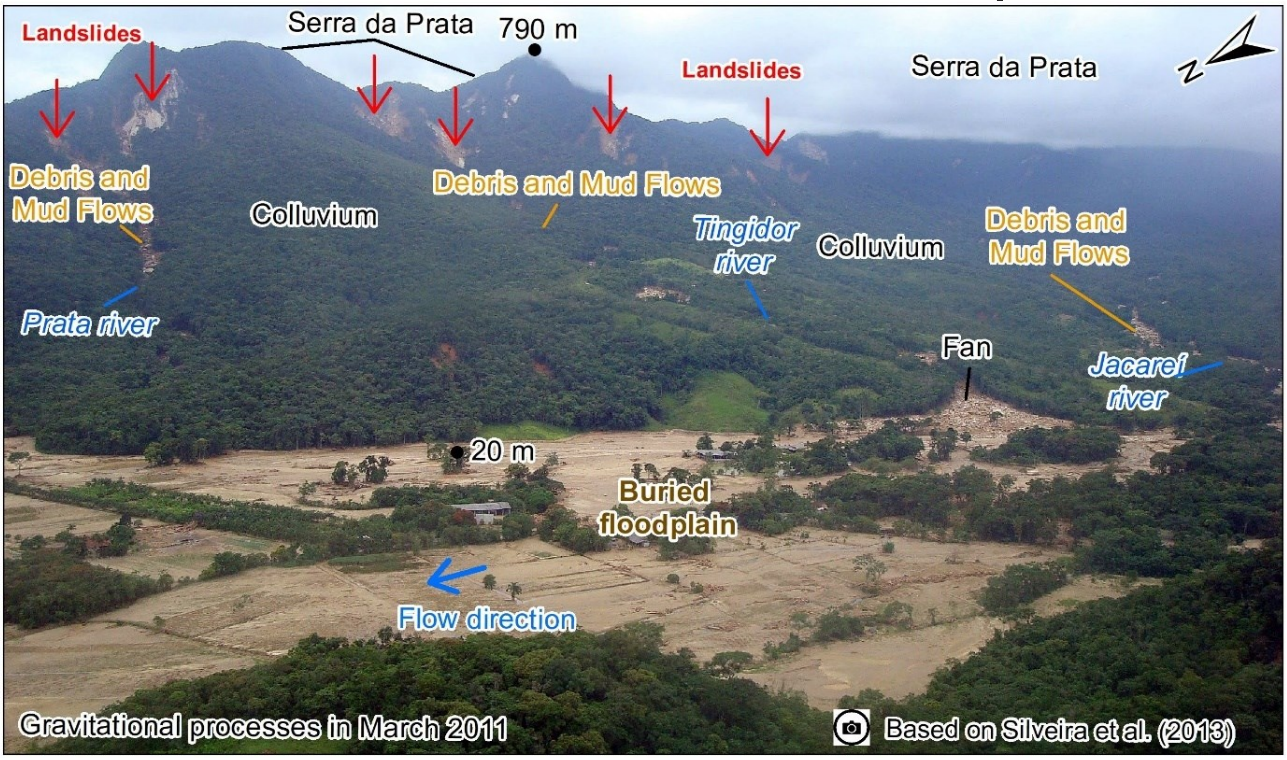

Source: The authors (2022).

The material was transported through the intramontane valleys in the form of mud and debris flows until it entered the alluvial plain of the Jacareí River (Figure 3 – A and B), where it was dammed by the BR 277 highway embankment (PINTO et al.; 2014; SILVEIRA et al., 2014) (Figure 2 and Figure 3 - C). The widespread flooding of the plain and the accumulation of wood logs resulted in the rupture of the BR 277 bridge over the Jacareí River (Figure 2 and Figure 3 – C and D).

Figure 3 – A: Landslides in the upper third of the slopes of the Serra da Prata. B: Intramontane channels after the passage of debris flows. C: BR 277 highway bridge over the Jacareí River after the 11/03/2011 event. D: Alluvial plain of the Jacareí River buried by the mud flows of 11/03/2011.

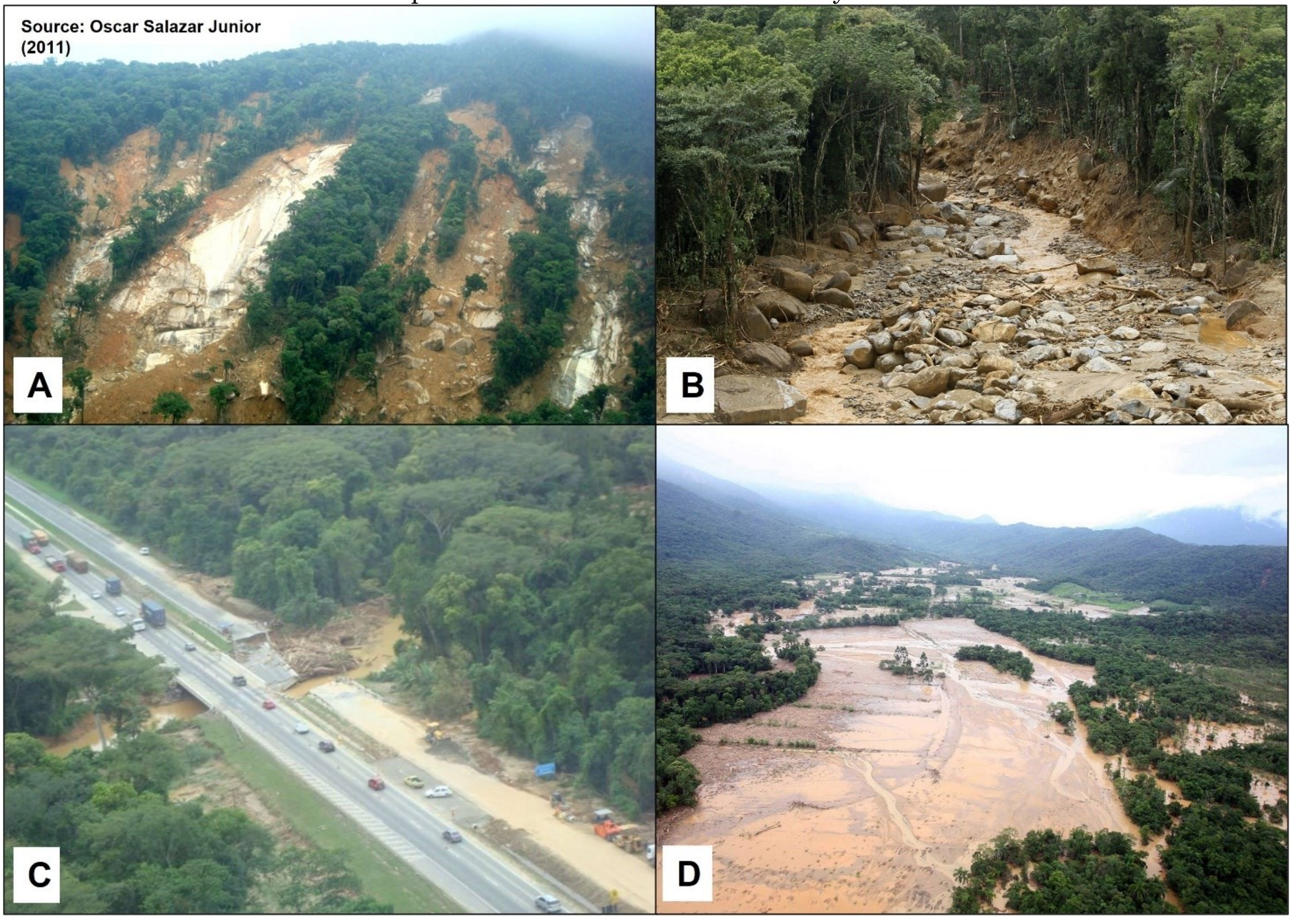

Sources: A: SALAZAR JUNIOR (2011a). B: KISSNER (2011). C: SALAZAR JUNIOR (2011b). D: MACHADO (2011).

Geospatial data and mapping of deposits and flow lines

A digital terrain model (MDT) with 2.5 meters of spatial resolution was acquired, generated from a survey by Synthetic Aperture Radar interferometry (SAR) between 2015 and 2016, made available by the Instituto Água e Terra (IAT) which is the state agency responsible for the environmental management of the State of Paraná. A panchromatic orbital image recorded by the WorldView-1 satellite on 02/05/2011 with a spatial resolution of 0.5 meters was also acquired, provided by the Secretaria Municipal de Meio Ambiente de Paranaguá (SEMMA), which is the municipal department responsible for the environmental management of the city of Paranaguá These data represented the most accurate image of the study area closest to the extreme event of March 11, 2011.

The study area was delimited with the aid of the aforementioned MDT. The slope was calculated in degrees from Horn's directional variables, through the slope tool of ArcGIS 10.4.1 (HORN, 1981). Subsequently, the average slope in the radius of 5 m was obtained with the ArcGIS focal statistics tool. The scope for analysis was defined considering the area between the 30-meter elevation (place where the Jacareí River enters the alluvial plain) to the BR 277 highway embankment, limited laterally by an average slope of up to 7 degrees, a value defined from the of field observations.

The identification of deposits was carried out considering inference regarding the granulometry of the material from the orbital image (Table 1) and consultation of the literature. (CHRISTOFOLETTI, 1981; STEVAUX; LATRUBESSE, 2017; MAGALHÃES JÚNIOR; BARROS, 2020). After identification in the orbital image, the deposits were vectorized in ArcMap, with a screen scale set at 1:2.000.

Table 1 - Depositions mapped in the alluvial plain of the Jacareí River in 2011.

Class	Subclass/Description		Criteria	Example
Pelitic deposits	Fine-grained material in portions of the floodplain not altered by the 2011 flood.		Absence of sedimentary material on the surface. Proximity to the slopes.	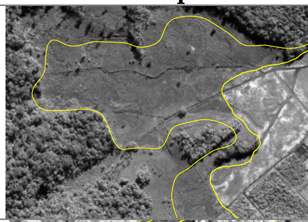
Psephytic deposits	Coarse-grained material (gravel). Consist of depositional fans and other points that debris flows reached.		Coarse material on the surface. Found in the upstream portions of the plain and in the mouths of the Prata and Tingidor rivers with a conical shape.	
Psammitic deposits	**Crevasse splay**	Overflow deposition. Resulting from the rupture of banks due to the obstruction of the river channel.	Located on the edge of the canal. Conical shape.	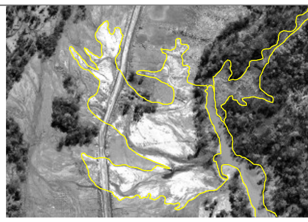
	River bar	Central or marginal deposits to the anastomosing channel formed by the event	Areas with sandy material located on the margins or in the center of the anastomosed canal.	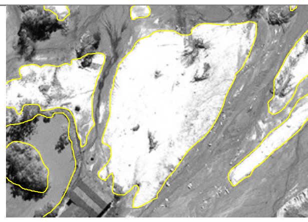
	Anastomosed riverbed	Anastomosed-type riverbed formed by the 2011 flood	Sandy material of darker tones, indicating moisture. Limited by debris deposits and flows.	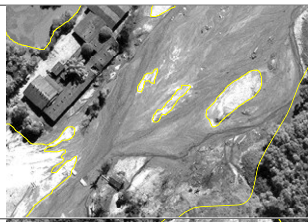
	Buried plain	Deposit formed by the 2011 flood. It covers an extensive area of the plain.	Surfaces with sandy material and areas of wet looking vegetation.	

Source: SEMMA (2019) and The authors (2022).

Areas not affected by the event were classified as pelitic (fine) deposits, considering granulometry predominantly in silt and clay, as described in a previous study (PAZ; PAULA, 2021). Psephytic deposits (gravel) were identified by observing the presence of coarse material in the orbital image. Psammitic deposits (sands) were identified considering the material on the surface and the wet aspect of the vegetation (affected by the flood), being subdivided into classes according to landscape position and morphology.

To analyze the direction of water and sediment currents during the flooding and after the breakage of the BR 277 bridge, flow lines were mapped through photointerpretation of the 2011 WorldView-1 orbital image (SEMMA, 2019). Through GIS, marks or scars in the sedimentary material left by the event were identified (Table 2). Then, arrows of varying length were inserted in order to infer the angle and direction of flow.

Table 2 - Examples of the mapping of the flow lines.

Scars	**Maps**
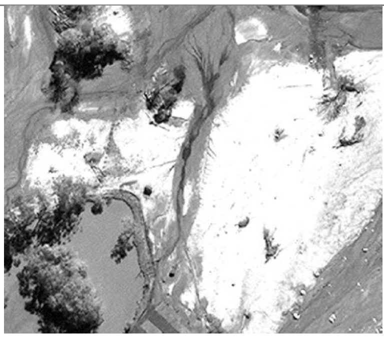	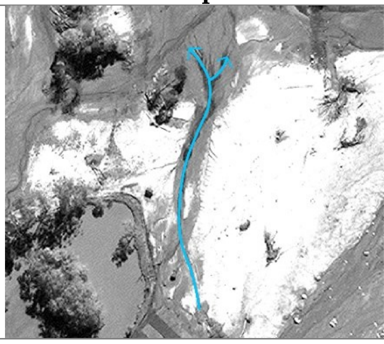
Scars	**Maps**
	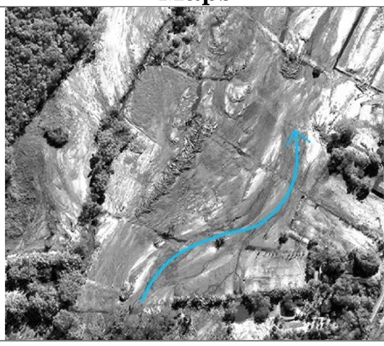

Source: The authors (2022).

Field surveys and sedimentology

Trenches were opened (manually or with machinery) and drills were carried out with a Dutch auger with a 20 cm bucket and a 6 cm mouth, only in the pelitic and psammitic deposits. The sampling in the pelitic deposits were carried out to understand the plain before 2011. The collections in the psammitic deposits were carried out to understand the sedimentology and estimate the volume of material transported by the mud flows, located exclusively in the alluvial plain. Samplings were not carried out in the psephytic deposits due to methodological incompatibility and, mainly, because these deposits extend from the plain to the intramontane channels, outside the study area. The 21 field surveys were carried out between 2019 and 2021. Of the 111 sampling points, 108 were used for volumetric reconstitution and in 19 for sedimentological analysis.

The deposits formed in 2011 (psammitic) were identified in the field, considering the criteria presented by Paz and Paula (2021): sandy layer in a massive structure of yellowish colors abruptly superimposed on the layer with fine material of tan to greyish colors, which may have buried roots. After identifying the event deposit, its total thickness was measured, and material was collected at a depth of 25 cm. The collection of material in the unaffected areas was also carried out at a depth of 25 cm.

The samples were dried in an oven at 50º for 72 hours. The granulometry was obtained through the integration between the methods of mechanical sieving and laser dispersion, using the Wentworth scale. The equipment used in the laser analysis was the *Bluewave* MICROTRAC. Due to equipment limitations, it was necessary to separate material larger than 2 mm (granules), and the samples were submitted to mechanical sieving (2 mm sieve), obtaining the percentage of granules in the sample. The rest of the sample was homogenized and ≅ 2 g was applied to the wet method of the *Bluewave* MICROTRAC equipment, obtaining a granulometric distribution between 0.02 and 2.000 µm (clay to very coarse sand). To integrate the results of both methods, it was necessary to adjust the percentages of each class on the Wentworth scale using the equation below:

$$PF\ (\%) = \frac{(100 - PG) \times PC}{100}$$

PF = Final percentage of the granulometric class in the integrated granulometry (sieve + laser);
PG = Percentage of granules measured by mechanical sieving;

PC = Percentage of the granulometric class calculated with laser scattering results.
Source: The authors (2022).

The granulometric distribution data were transferred to the SYSGRAN 3.0 software (CAMARGO, 2006), where the Folk and Ward granulometric parameters were calculated: mean, median, degree of selection, asymmetry, and kurtosis. The texture was identified according to the textural triangle adapted from the Soil Survey Manual (SANTOS et al., 2015).

The morphological properties of the material in the sand granulometric fractions (0 phi/φ to 4 phi/φ) were analyzed using a pocket magnifying glass with a 20X magnification, comparing with sphericity and roundness charts (MANCINI, 2016). Finally, a bivariate correlation test was applied between the granulometric classes of the samples collected in Excel software (CORREL function).

Volumetric reconstitution of the deposits

Volumetric reconstitution was performed only in the psammitic deposits (which were formed in the event). The deposit thickness value was entered in the attributes table of the vector file of the collected points. The cloud of 108 points with the aforementioned thickness information was submitted to interpolation in the ArcGIS 10.4.1.

The interpolation algorithm used was the *Spline With Barriers*. This was chosen considering the spatial behavior of the collected data, where the type of deposit reflects the thickness characteristics. That is, abrupt thickness transitions were observed only by comparing the thicknesses in different deposits, while in the same deposit a certain homogeneity of values was observed, with slight variation. Therefore, it is considered that the minimum curvature of this algorithm, associated with barriers such as the limits of the previously mapped 2011 deposits, best fits the proposed volumetric estimate.

The resulting raster had 1 m of spatial resolution and was applied to the Surface Volume tool of ArcGIS 10.4.1 where, considering the reference plane below as zero, the volume of the psammitic deposits was estimated. To estimate the mass of the deposits, the volume was multiplied by the apparent density of the material, considered here at 1.5 mg/m³, an average value calculated for samples with a sand texture (BRADY; WEIL, 2013; ZERI et al., 2018).

RESULTS AND DISCUSSION

Psammitic deposits predominate in the floodplain (87.59%), being the largest floodplain subunit (76.12%), distributed between the upstream and downstream portions of the study area (Figure 4 and Table 3). The pelitic deposits are found at the lateral ends of the area and in vegetation fragments, areas not affected by the March 2011 flood. Psephytic deposits, resulting from debris flows, are found at the mouths of the Jacareí, Tingidor and Prata Rivers, where they formed fans (or dejection cones), extending to the intramontane channels. In these areas, clasts with a diameter greater than 150 cm are found, classified as boulders, being surrounded by blocks, pebbles, and granules. Except in the fan in the Rio de la Plata, where granules predominate.

Figure 4 - Deposits in the alluvial plain of the Jacareí River in 2011. Note that the fluvial channels in the plain are not illustrated in the figure due to their filling during the burial event by the mud flows in 2011.

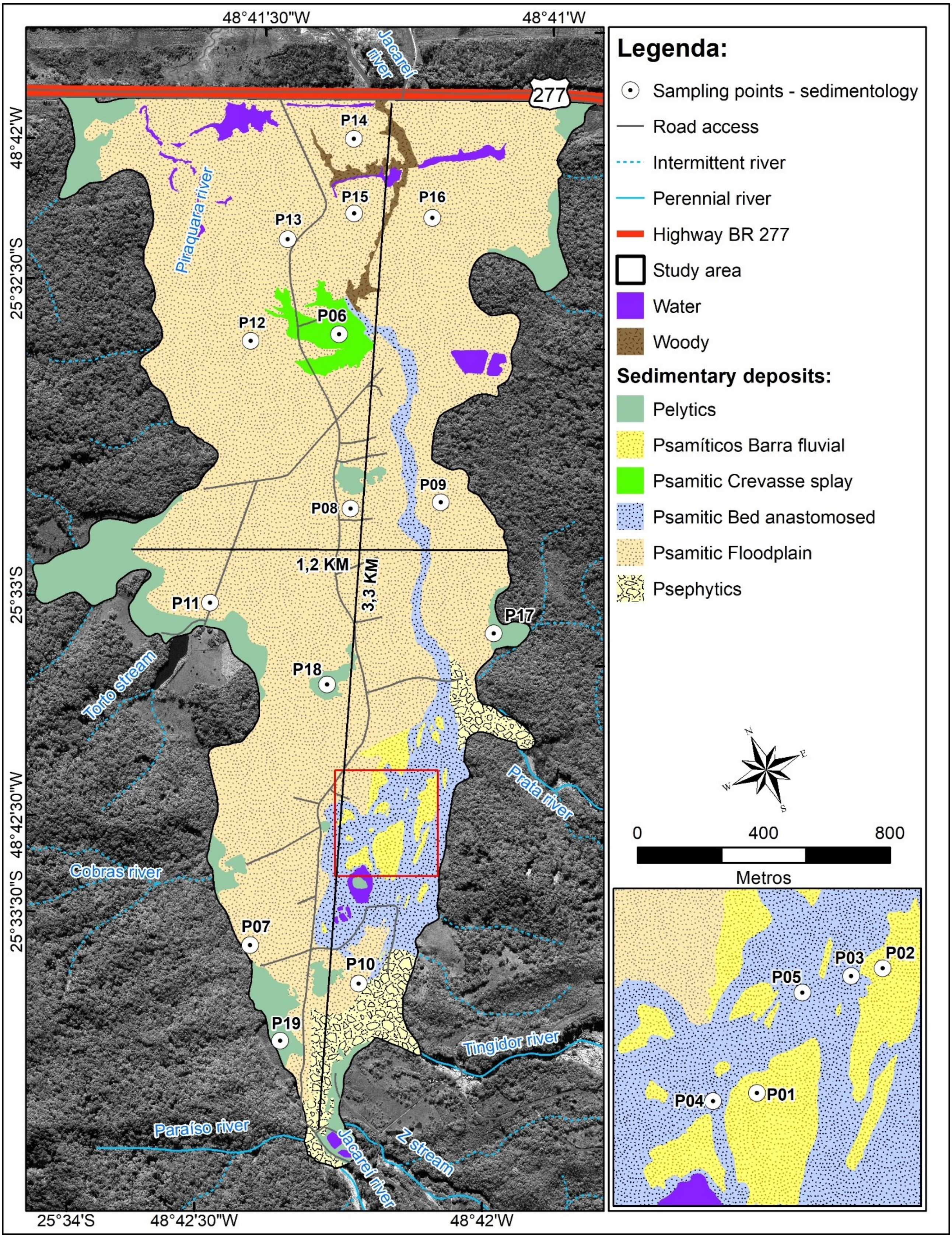

Source: The authors (2022).

Table 3 - Characteristics of the sedimentary units of the alluvial plain of the Jacareí River in 2011.

Units/Subunits		Area (ha)	Area (%)	Sector of the alluvial plain
Pelitic deposits		25,06	8,76	Distal portions
Psephytic deposits		10,45	3,65	River mouths – Upstream portion
Psammitic deposits	Breakthrough deposit	4,48	1,56	Downstream portion
	River bar	5,28	1,85	Upstream portion
	Anastomosed river bed	23,04	8,06	Upstream portion
	Flood plain	217,68	76,12	Upstream and downstream portion

Source: The authors (2022).

Mud flows ran through the alluvial plain (3.3 km long by 1.2 km wide) fostering widespread flooding in the area. The sedimentological description of the psammitic and pelitic deposits is presented in the following topic. In addition to clasts, several points with accumulation of woody material are identified in the orbital image, mainly in the bed of the Jacareí River near BR 277. Additionally, in this portion, several bodies of water formed by the event were also identified.

Sedimentology of deposits formed in 2011

The samples collected in the psammitic deposits were classified between fine sand (3 φ) and very fine sand (4 φ), and in most cases the peak of the histogram occurred in the medium sand class (2 φ), with the exception of P- 05, P-12 and P-16 (peak in fine sand – 3 φ). The psammitic subunits "river bar" and "anastomosed riverbed" had the highest sand contents (above 78%) (Figure 5). From a textural point of view, the samples from these units were classified as "free sand", with the exception of sample P-05 which was classified as "sand" (86.47% sand). In all psammitic samples, low sphericity, sub-angular to very angular clasts were found.

Figure 5 - Particle size frequency histogram for the samples P-01 to P-16.

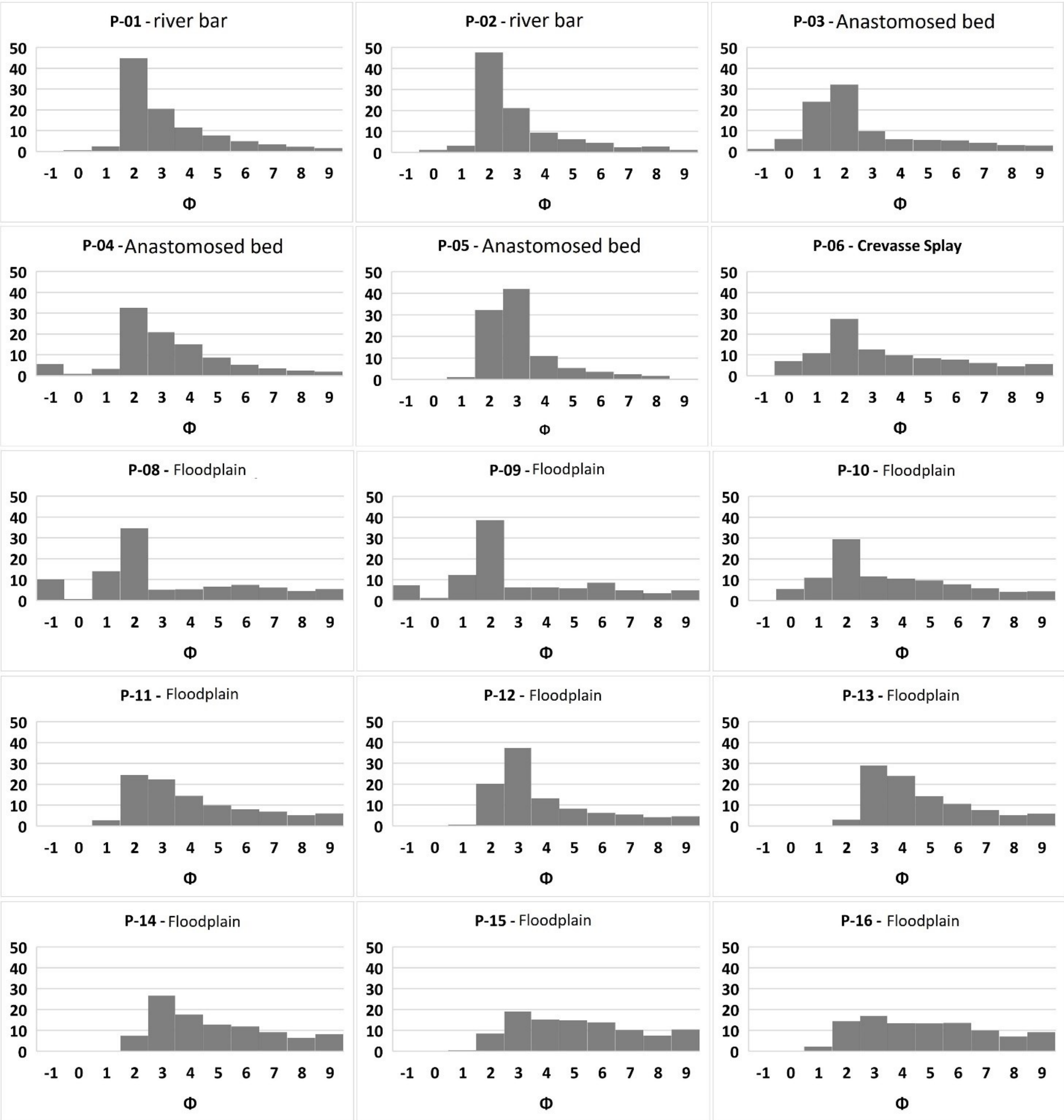

Source: The authors (2022). The x-axis is phi (φ) and the y-axis is percentage (%).

The material from the "breakthrough deposit" unit was classified as "sandy loam". Samples P-07 to P-14, collected in the buried floodplain, were also classified as "sandy loams". In these units, samples P-04, P-08 and P-09 were gravelly. Samples P-15 and P-16 recorded the lowest levels of sand in samples collected in psammitic deposits, classified as "free". Samples P-17 to P-19 refer to pelitic deposits, with the average diameter classified as "average silt" (Figure 6). The samples presented an average of 59% of the material in silt, resulting in the textural classification "loose silty".

Figure 6 - Particle size frequency histogram for samples P-17 to P-19.

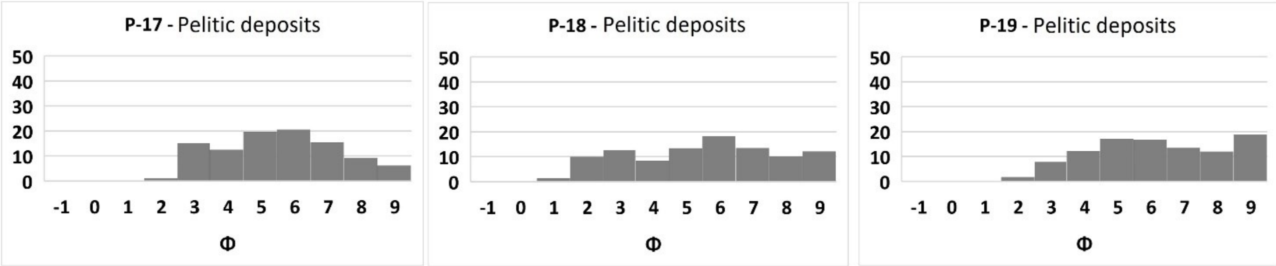

Source: The authors (2022). The x-axis is phi (φ) and the y-axis is percentage (%).

In addition to the mean diameter, the asymmetry parameter showed a significant difference between the psammitic and pelitic samples (Table 4). Psammitic samples were classified as "positive" to "very positive" asymmetry, while pelitic samples were classified as "approximately symmetrical".

Analyzing the bivariate correlation between the granulometric distribution of psammitic samples (Figure 7), two patterns of high positive correlation are observed: samples P-01 to P-12 ($\bar{x}$0.8) and samples P-13 to P-16 ($\bar{x}$0 ,9). The two groups identified show a weak positive correlation with each other ($\bar{x}$0.33), even though all samples were psammitic. On average, a very weak positive correlation was found between the pelitic and psammitic samples ($\bar{x}$0.15).

Table 4 - Granulometric statistical parameters of the collected samples.

Unit	Sample	Mean	Median	Selection	Asymmetry	Kurtosis
Psammitic deposits – River bar	P-01	2,64	2,10	1,66	0,56	1,11
	P-02	2,48	1,96	1,60	0,59	1,30
Psammitic deposits - Anastomosed riverbed	P-03	2,28	1,58	2,29	0,48	1,22
	P-04	2,74	2,37	2,04	0,24	1,37
	P-05	2,54	2,39	1,30	0,33	1,55
Psammitic deposits – Breakthrough deposit	P-06	3,09	2,39	2,57	0,38	0,95
Psamitic deposits - Flood plain	P-07	3,61	2,91	2,56	0,38	0,77
	P-08	2,71	1,73	2,71	0,50	0,93
	P-09	2,69	1,76	2,59	0,49	1,05
	P-10	3,04	2,35	2,42	0,40	0,95
	P-11	3,63	3,04	2,27	0,41	0,90
	P-12	3,42	2,78	2,00	0,51	1,17
	P-13	4,19	3,74	1,91	0,40	0,93
	P-14	4,36	3,91	2,15	0,32	0,85
	P-15	4,70	4,46	2,28	0,16	0,83
	P-16	4,40	4,23	2,37	0,13	0,82
Pelitic deposits	P-17	5,00	5,07	1,90	0,00	0,90
	P-18	5,07	5,23	2,41	-0,08	0,80
	P-19	5,78	5,66	2,11	0,02	0,79

Source: The authors (2022).

Figure 7 - Bivariate correlation matrix between the granulometric distributions of the psammitic samples collected.

Psamitic

Samples	P1	P2	P3	P4	P5	P6	P7	P8	P9	P10	P11	P12	P13	P14	P15	P16
P1	1,00	1,00	0,74	0,97	0,84	0,94	0,93	0,80	0,87	0,94	0,90	0,70	0,24	0,36	0,33	0,60
P2	1,00	1,00	0,76	0,96	0,83	0,94	0,93	0,82	0,89	0,94	0,87	0,69	0,19	0,31	0,28	0,55
P3	0,74	0,76	1,00	0,64	0,49	0,88	0,79	0,86	0,87	0,88	0,50	0,30	-0,19	-0,11	-0,15	0,15
P4	0,97	0,96	0,64	1,00	0,89	0,86	0,84	0,71	0,78	0,87	0,93	0,79	0,40	0,49	0,41	0,63
P5	0,84	0,83	0,49	0,89	1,00	0,73	0,66	0,45	0,53	0,69	0,92	0,96	0,58	0,68	0,53	0,66
P6	0,94	0,94	0,88	0,86	0,73	1,00	0,94	0,81	0,88	0,99	0,80	0,58	0,13	0,24	0,23	0,52
P7	0,93	0,93	0,79	0,84	0,66	0,94	1,00	0,86	0,91	0,96	0,81	0,53	0,09	0,25	0,31	0,61
P8	0,80	0,82	0,86	0,71	0,45	0,81	0,86	1,00	0,99	0,84	0,52	0,23	-0,28	-0,16	-0,13	0,20
P9	0,87	0,89	0,87	0,78	0,53	0,88	0,91	0,99	1,00	0,90	0,61	0,32	-0,19	-0,07	-0,03	0,30
P10	0,94	0,94	0,88	0,87	0,69	0,99	0,96	0,84	0,90	1,00	0,80	0,54	0,11	0,22	0,23	0,52
P11	0,90	0,87	0,50	0,93	0,92	0,80	0,81	0,52	0,61	0,80	1,00	0,90	0,63	0,73	0,69	0,85
P12	0,70	0,69	0,30	0,79	0,96	0,58	0,53	0,23	0,32	0,54	0,90	1,00	0,76	0,84	0,70	0,76
P13	0,24	0,19	-0,19	0,40	0,58	0,13	0,09	-0,28	-0,19	0,11	0,63	0,76	1,00	0,97	0,89	0,76
P14	0,36	0,31	-0,11	0,49	0,68	0,24	0,25	-0,16	-0,07	0,22	0,73	0,84	0,97	1,00	0,95	0,87
P15	0,33	0,28	-0,15	0,41	0,53	0,23	0,31	-0,13	-0,03	0,23	0,69	0,70	0,89	0,95	1,00	0,94
P16	0,60	0,55	0,15	0,63	0,66	0,52	0,61	0,20	0,30	0,52	0,85	0,76	0,76	0,87	0,94	1,00

-0.39 a -0.20 Weak negative
-0.19 a 0.00 Very weak negative
0.00 a 0.19 Very weak positive
0.20 a 0.39 Weak positive
0.40 a 0.69 Positive moderate
0.70 a 0.89 Strong positive
0.90 a 1.00 Very strong positive
Group 1
Group 2

Source: The authors (2022).

Samples P-01 to P-12 are located in the upstream and middle portions of the floodplain, while samples P-13 to P16 are located in the downstream portion (near the BR 277 highway). The mapping of the flow lines (Figure 8) indicates two main directions of water and sediments during the event, both of which start at the point where the Jacareí River enters the alluvial plain and are close to the BR 277 highway. The first flows close to the slopes of the Serra da Prata, following the anastomosed riverbed until the rupture deposit. The second flows near the slopes to the west, entering the vicinity of the Piraquara River.

Figure 8 - Main granulometric parameters and flow lines in the alluvial plain of the Jacareí River in 2011. Note that, after the mud flow event and the consequent of burial of the alluvial plain, it is not possible to identify the fluvial channels due to their filling. It is only possible to observe the anastomosed channel imposed on the Jacareí river.

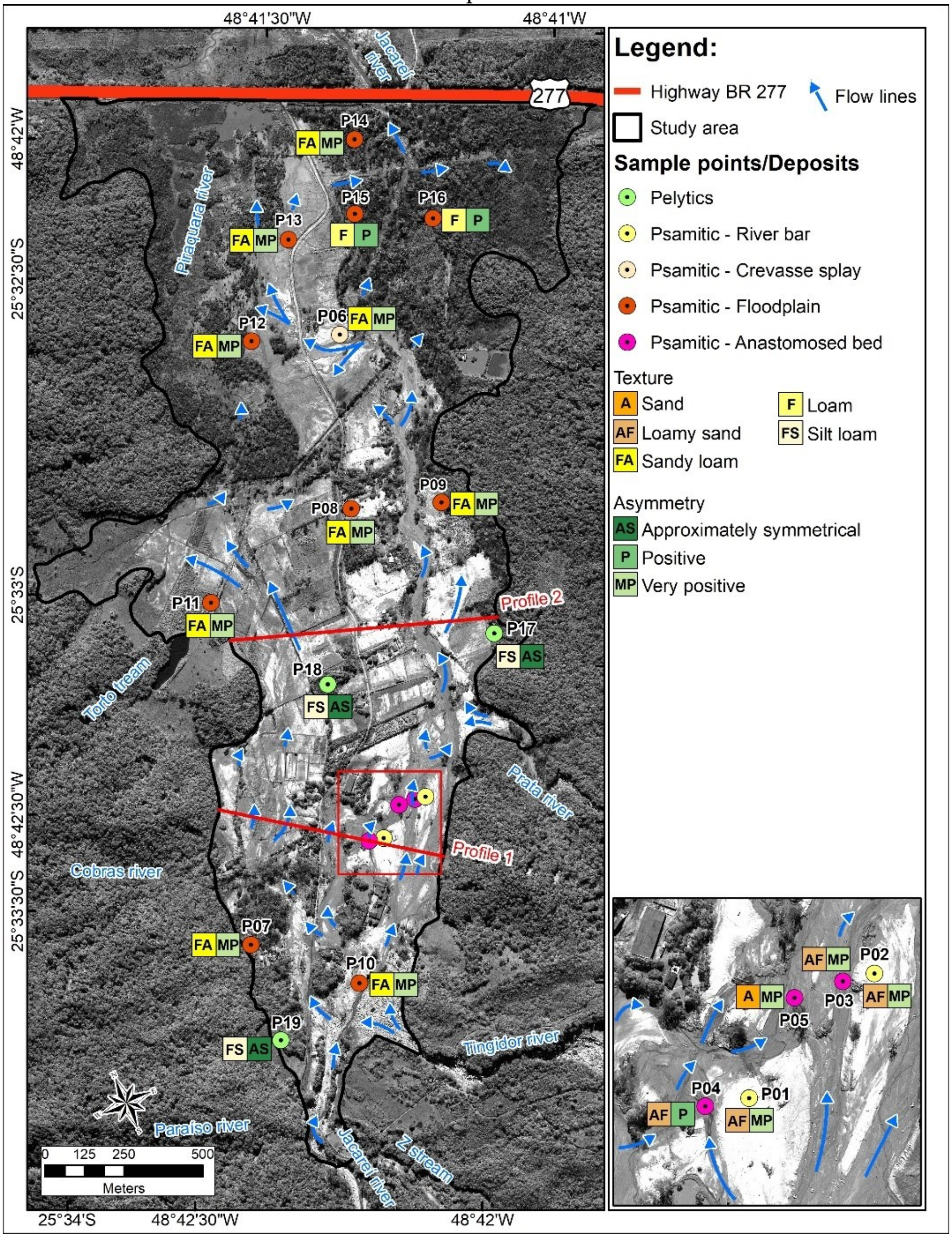

Source: The authors (2022).

Volumetric reconstruction

The 108 sampling points showed values ranging from 20 cm, at the lateral ends of the alluvial plain, to 120 cm, in a river bar surrounded by the anastomosed bed. The average thickness was 50 cm. The total volume of psammitic deposits was estimated at 1.134.699,28 m³, equivalent to 1,7 million tons of sediment. To better analyze the distribution of deposits in the plain, the generated model was divided into classes (Table 6). Transects were traced over the plain in order to observe the longitudinal variation of the deposits (Figure 9).

Table 6 - Area (hectare and percentage) of each thickness class in the floodplain.

Class	Area (hectare)	Area (%)
Between 20 and 35 cm	60,3001	24,09
Between 35 and 45 cm	69,8435	27,89
Between 45 and 55 cm	83,4906	33,35
Between 55 and 75 cm	31,9649	12,76
Between 75 and 120 cm	4,7813	1,91

Source: The authors (2022).

Figure 9 - Transects illustrating the vertical variation in deposit thickness.

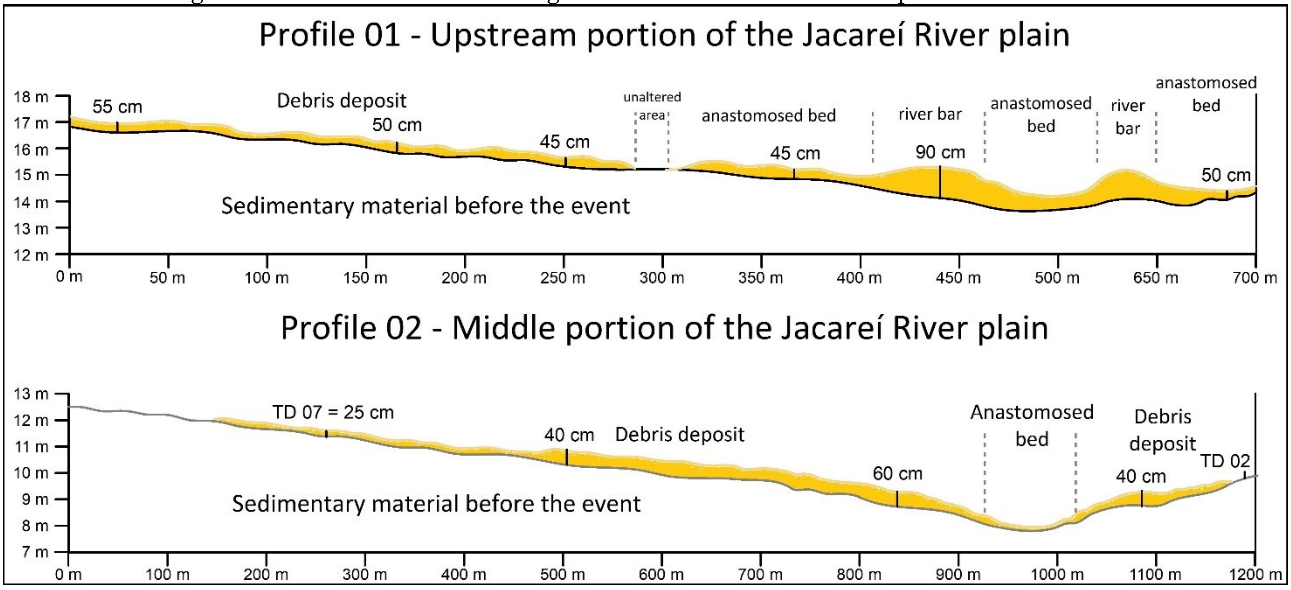

Source: The authors (2022).

According to the generated model (Figure 10), there is a concentration of deposited volumes at three points: 1 - close to the Jacareí river channel throughout the plain; 2 – in the upstream sector, shortly after the arrival of the Jacareí River on the plain; 3 – in the downstream sector, right after the rupture deposit formed on the banks of the Jacareí river channel. In the lateral extremities of the plain and in the anastomosed riverbed, the smallest values of thickness (< 35 cm) were observed.

Figure 10 - Thickness model of psammitic deposits.

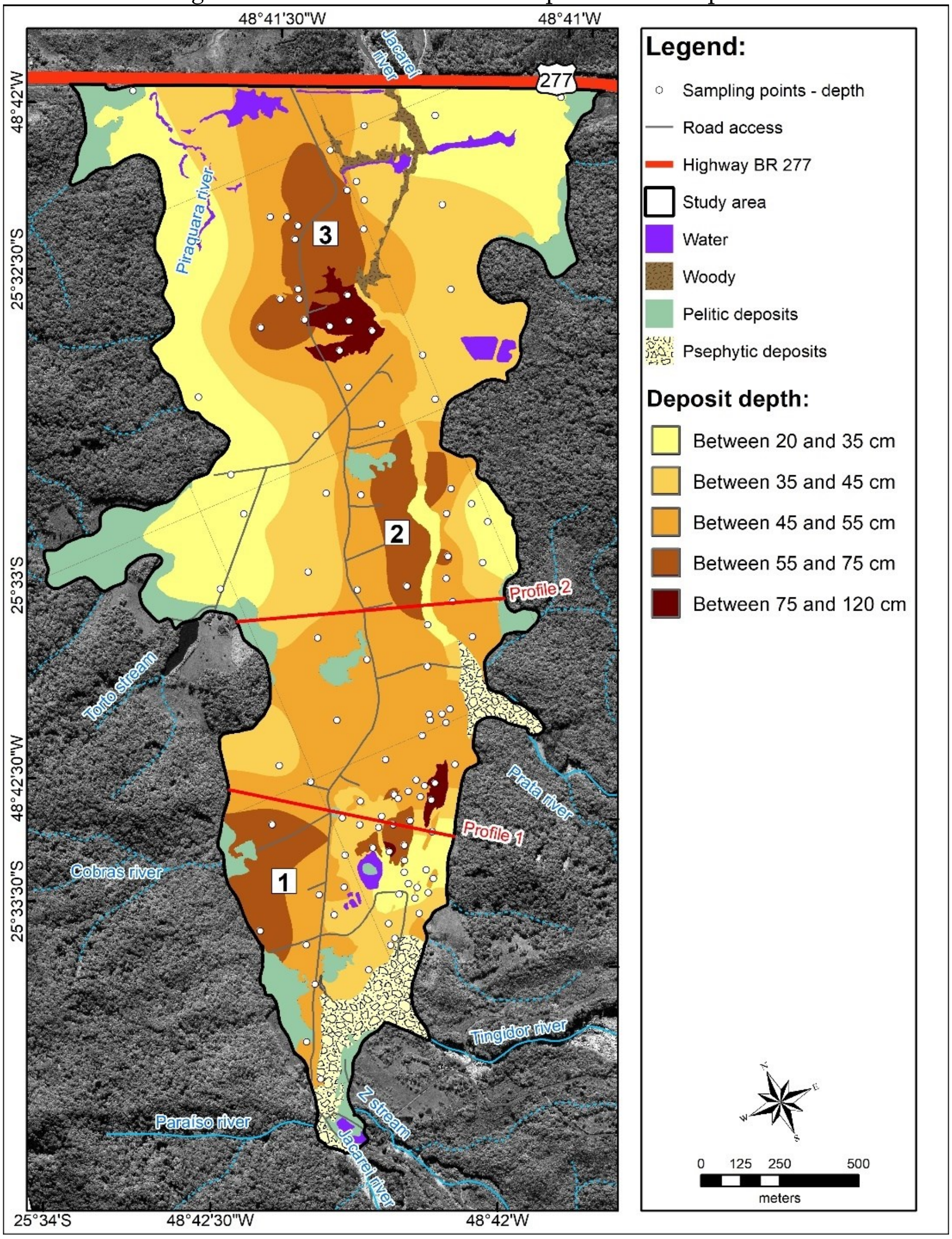

Source: The authors (2022).

DISCUSSION

The results obtained indicate two stages in the construction process of the psammitic deposits in 2011. The first refers to the arrival and spreading of sedimentary material, woody material and water in the alluvial plain, originating from the flows of mud and debris between 14h and 15h on 11/03/2011 (according to reports presented by residents), burying the past surface.

The flow across the BR 277 bridge was interrupted due to the accumulation of wood logs. The BR 277 highway embankment worked as a dam, accumulating water and sediment on the plain. The first two sediment volume concentration points (near the Jacareí river channel and in the upstream sector, shortly after the arrival of the Jacareí river in the plain) were formed at this stage.

The second stage began around 19h, when the BR 277 highway bridge breaks (ECOVIA, 2011). Water and sediments flow into the Antonina Bay, shaping the newly accumulated material on the plain. The anastomosed riverbed originates from erosion caused by the flow of runoff. On the other hand, the rupture deposit (*crevasse splay*) originates from the clogging of the Jacareí channel by woody material and consequent rupture, resulting in the deposition of material carried from the anastomosed bed. This interpretation is supported by the analysis of flow lines. The third sediment volume concentration point (in the downstream sector) was formed at this stage, fed by the rupture deposit.

The existence of two groups in the psammitic samples is explained by this dynamic. Finer material that was in the anastomosed riverbed was transported to the downstream portion of the plain. This explains the significant texture difference within the psammitic samples (sand to loam and sandy loam to loam). As for asymmetry, positive asymmetry curves are often associated with depositional moments, while approximately symmetrical curves suggest a combination of erosion and deposition processes (FRIEDMAN, 1961; DUANE, 1964).

The results obtained confirm the low textural maturity (immaturity) of the psammitic material in the alluvial plain of the Jacareí River. These are poorly selected sediments, with the presence of fine and angular clasts of low sphericity (FELIX; HORN FILHO, 2020). This result is in agreement with the literature, and this behaviour is expected in material generated by mud and debris flows (HUNGR, 2005; REGMI et al., 2015).

In order to understand the dimension of the event, it is relevant to compare the estimated mass of the psammitic sedimentary packages formed in 2011 (1,7 million tons) with the measured values of sediment production in the JRB and surroundings. Considering the regional context, the estimated mass of psammitic deposits here is more than 8.5 times the estimated total sediment production for all hydrographic units (basins + island systems) that drain into the Paranaguá Estuarine Complex (PEC), with a volume estimated at 197.017,21 tons per year (RUTYNA et al., 2021). It should be noted that the volume estimate presented here is part of the psammitic deposits in the alluvial plain, with psephytic material in the plain and in the fans and intramontane channels.

Considering the volume estimated here, it is possible to classify the event that occurred in the Jacareí river basin as of high magnitude, partially within class 7 (106 - 107 m^3) according to the proposal by Jakob (2005) (only considering the volume of material). Class 7 mass runs can destroy structures and parts of cities, in addition to obliterating valleys, fans, plains and river channels for tens of kilometers (JAKOB, 2005). Had it not been for the BR 277 embankment, the mud flows could have reached further downstream parts of the Jacareí River plain.

The alluvial plain of the Jacareí River should be seen as a sedimentary stock, a source area of material in the hydro-sedimentary cycle of the landscape. The sediments in this area are unconsolidated and can be eroded by the river, even more so in cases of extreme rainfall events. Despite the predominance of the sand fraction, the sedimentary material formed in 2011 presents significant values of silt ($\bar{x}$ 28%), the predominant granulometric fraction in the material dredged in the navigation channels of the ports of Antonina and Paranaguá (BOLDRINI; PAULA, 2009). Thus, the material eventually eroded and transported by the river, can contribute to the problem of sedimentation in the bay of Antonina (PAULA, 2010,; PAULA,2016).

CONCLUSION

The gravitational processes of landslides and mud and debris flows in the Jacareí river basin in 2011 resulted in psammitic and psephytic deposits that covered about 91% of the alluvial plain. Psammitic deposits were the most expressive (≅ 88%), classified as loam to sandy loam, estimated at 1,7 million tons of sediments.

The results demonstrate the high magnitude of the 2011 event, since in a period of less than 24 hours the JRB moved more than 8,5 times the annual production of sediments from the hydrographic units that drain to the Paranaguá Estuarine Complex. The transformations in the alluvial plain of the Jacareí River reflect the genetic processes of terrigenous origin in the coastal plain.

Additional studies are recommended that address the volume of psephytic deposits from intramontane channels to the alluvial plain. The results presented here may have ramifications in public policy actions, mainly in the territorial planning of this landscape. The new environmental dynamics reveal new weaknesses, such as areas that are sources of sedimentary material, and potentialities, considering that the contribution of sedimentary material can renew the fertile character of the soil, providing opportunities for economic activities in the area.

ACKNOWLEDGMENT

This paper is part of the first author's doctoral thesis. To the Laboratório de Geoprocessamento e Estudos Ambientais (LAGEAMB) of UFPR. To the Laboratório de Biogeografia e Solos (LABS) of UFPR. To the Centro de Pesquisas Aplicadas em Geoinformação (CEPAG) of UFPR. To the Laboratório de Análises de Minerais e Rochas (LAMIR) of UFPR. To the Laboratório de Estudos Costeiros (LECOST) of UFPR.

REFERENCES

ANGULO, R. J. Mapa do Cenozóico do litoral do Estado do Paraná. **Boletim Paranaense de geociências**, v. 55, n. 1, p. 25–42, 2004. http://dx.doi.org/10.5380/geo.v55i0.4281

ESRI. ArcGIS 10.4.1. 2016. Versão estudante. Available: https://desktop.arcgis.com/en/arcmap/10.4/get-started/setup/arcgis-desktop-quick-start-guide.htm. Access on: May 19, 2021.

AVILA-DIAZ, A.; BENEZOLI, V.; JUSTINO, F.; TORRES, R.; WILSON, A. Assessing current and future trends of climate extremes across Brazil based on reanalyses and earth system model projections. **Climate Dynamics**, v. 55, n. 5, p. 1403–1426, 2020. https://doi.org/10.1007/s00382-020-05333-z.

ÁVILA, A.; JUSTINO, F.; WILSON, A.; BROMWICH, D.; AMORIM, M. Recent precipitation trends, flash floods and landslides in southern Brazil. **Environmental Research Letters**, v. 11, n. 11, p. 114029, 2016. http://dx.doi.org/10.1088/1748-9326/11/11/114029.

BOLDRINI, E. B.; PAULA, E. V. **Gestão Ambiental Portuária: Subsídio para o licenciamento das Dragagens**. 1. ed. Antonina: ADEMADAN, 2009.

BORGA, M.; STOFFEL, M.; MARCHI, L.; MARRA, F.; JAKOB, M. Hydrogeomorphic response to extreme rainfall in headwater systems: Flash floods and debris flows. **Journal of Hydrology**, v. 518, p. 194–205, 2014. https://doi.org/10.1016/j.jhydrol.2014.05.022

BRADY, N. C.; WEIL, R. R. Arquitetura e propriedades físicas do solo. In: BRADY, N. C.; WEIL, R. R. (Eds.). **Elementos da Natureza e Propriedades dos Solos**. Porto Alegre: Bookman, 2013. p. 106-145.

BIGARELLA, J. J. Movimentos de massa. In: **Estrutura e origem das paisagens tropicais e subtropicais**. Volume 3 ed. Florianópolis: Editora da UFSC, 2003. p. 1024–1098.

CAMARGO, M. G. SYSGRAN: um sistema de código aberto para análises granulométricas do sedimento. **Revista Brasileira de Geociências**, v. 36, n. 2, p. 371–378, 2006. https://doi.org/10.25249/0375-7536.2006362371378

COSTA, J. E. Physical Geomorphology of Debris Flows. In: COSTA, J. E.; FLEISHER, P. J. (Eds.). **Developments and Applications of Geomorphology**. Berlin, Heidelberg: Springer Berlin Heidelberg, 1984a. p. 268–317. https://doi.org/10.1007/978-3-642-69759-3_9

CHRISTOFOLETTI, A. **Geomorfologia fluvial**. 1. ed. São Paulo: Edgard Blucher, 1981.

DUANE, D. B. Significance of skewness in recent sediments, western Pamlico Sound, North Carolina. Journal of Sedimentary Research, v. 34, n. 4, p. 864–874, 1964. Available: https://pubs.geoscienceworld.org/sepm/jsedres/article-abstract/34/4/864/95805/Significanceof-skewness-in-recent-sediments?redirectedFrom=PDF Access on: August 12, 2020.

ECOVIA **@ecovia**. BR 277 - Alagamento da Ponte Jacareí, no Km 18, interdita totalmente as pistas. Não paginado. Available: https://twitter.com/ecovia/status/46297826665312256. Access on: January 26, 2021.

FACURI, G. G.; PICANÇO, J. L. Evaluationas and proposals for the debris flow hazard mapping method of the GIDES Project. **Landslides**, v. 18, n. 1, p. 339–352, 2021. https://doi.org/10.1007/s10346-020-01480-w.

FELIX, A.; HORN FILHO, N. O. Propriedade dos Sedimentos. In: **Apostila Sedimentologia**. 1. ed. Florianópolis: Universidade Federal de Santa Catarina, 2020. p. 29–39. Available: https://geocost.ufsc.br/. Access on: January 26, 2022.

FRIEDMAN, G. M. Distinction between dune, beach, and river sands from their textural characteristics. **Journal of Sedimentary Research**, v. 31, n. 4, p. 514-529, 1961. Available: https://pubs.geoscienceworld.org/sepm/jsedres/articleabstract/31/4/514/95526/Distinction-between-dune-beach-and-riversands?redirectedFrom=PDF Access on: May 11, 2022.

FROUDE, M. J.; PETLEY, D. N. Global fatal landslide occurrence from 2004 to 2016. **Natural Hazards and Earth System Sciences**, v. 18, n. 8, p. 2161–2181, 2018. https://doi.org/10.5194/nhess-18-2161-2018

GRAMANI, M. F. CORRIDAS DE MASSA NA SERRA DA MANTIQUEIRA: DESCRIÇÃO E AVALIAÇÃO DA OCORRÊNCIA NO CÓRREGO DO BRAÇO. **Revista Técnico-Científica do CREA-PR**, v. Spe., p. 15, 2018. Available: http://creaprw16.crea-pr.org.br/revista/sistema/index.php/revista/article/view/387. Access on: February 28, 2022.

HORN, B. K. P. Hill shading and the reflectance map. **Proceedings of the IEEE**, v. 69, n. 1, p. 14–47, 1981. https://doi.org/10.1109/PROC.1981.11918

HUNGR, O. Classification and terminology. In: JAKOB, M.; HUNGR, O. (Eds.). **Debris-flow Hazards and Related Phenomena**. Berlin, Heidelberg: Springer Berlin Heidelberg, 2005. p. 9–23. https://doi.org/10.1007/3-540-27129-5_2.

HUNGR, O.; LEROUEIL, S.; PICARELLI, L. The Varnes classification of landslide types, an update. **Landslides**, v. 11, n. 2, p. 167–194, 2014. https://doi.org/10.1007/s10346-013-0436-y

IAT - Instituto Água e Terra. **Base planialtimétrica da porção central do litoral do Paraná**. Curitiba, 2016. Available: https://www.iat.pr.gov.br/. Access on: February 28, 2022.

INAPAR - Instituto das Águas do Paraná. **Base hidrográfica do estado do Paraná na escala 1:50.000**. 2012. Available: https://www.abrhidro.org.br/SGCv3/publicacao.php?PUB=3&ID=81&SUMARIO=1228. Access on: February 28, 2022.

IBGE - Instituto Brasileiro de Geografia e Estatística. Malha municipal. Rio de Janeiro, 2012. Available: https://www.ibge.gov.br/geociencias/organizacao-do-territorio/malhas-territoriais/15774-malhas.html?=&t=downloads. Access on: February 28, 2022.

KISSNER, O. **Rio Jacareí após os deslizamentos**. Agência Estadual de Noticiais do Paraná. 2011. 1 fotografia, color.

JAKOB, M. A size classification for debris flows. **Engineering Geology**, v. 79, n. 3, p. 151–161, 2005. https://doi.org/10.1016/j.enggeo.2005.01.006

KOBIYAMA, M.; MICHEL, G. P.; ENGSTER, E. C.; PAIXÃO, M. A. Historical analyses of debris flow disaster occurrences and of their scientific investigation in Brazil. **Labor e Engenho**, v. 9, n. 4, p. 76–89, 2015. https://doi.org/10.20396/lobore.v9i4.8639477

KUMARI, S.; CHAUHAN, A.; SHANKAR, V. Assessment of climate change implications on landslides in mid and high hills of Himachal Pradesh, India. **Arabian Journal of Geosciences**, v. 14, n. 14, p. 1323, 2021. Available: https://doi.org/10.1007/s12517-021-07668-1.

LI, Y.; WANG, B.; ZHOU, X.; GOU, W. Variation in grain size distribution in debris flow. **Journal of Mountain Science**, v. 12, n. 3, p. 682–688, 2015. https://doi.org/10.1007/s11629-014-3351-3

MACHADO, R. **Vista em sobrevoo da comunidade de florestas após os movimentos de massa.** SECJ. 2011. 1 fotografia, color.

MAGALHÃES JÚNIOR, A. P.; BARROS, L. F. P. Depósitos fluviais e feições deposicionais. In: MAGALHÃES JÚNIOR, A. P.; BARROS, L. F. P. (Eds.). **HIDROGEOMORFOLOGIA: Formas, processos e registros sedimentares fluviais**. Rio de Janeiro: Bertrand Brasil, 2020. p. 259–278.

MANCINI, F. Mapeamento e Reconhecimento de Rochas Sedimentares. In: NADALIN, R. J. (Ed.). **Tópicos Especiais em Cartografia Geológica**. Curitiba: Departamento de Geologia - UFPR, 2016. p. 181–204.

MINEROPAR – Minerais do Paraná. **Atlas geológico do Estado do Paraná - Folha de Curitiba (SG-22-X-D) MINERAIS DO PARANÁ AS.** Curitiba, 2006. Available: https://www.iat.pr.gov.br/Pagina/Mapeamento-Geologico. Access on: January 26, 2022.

MINEROPAR - Minerais do Paraná. **MAPEAMENTO GEOLÓGICO--GEOTÉCNICO DA PORÇÃO LESTE DA SERRA DO MAR DO ESTADO DO PARANÁ**. 1. ed. 102p. 2011. Curitiba. Available: https://www.documentador.pr.gov.br/documentador/pub.do?action=d&uuid=@gtf-escriba-minerop@26e14cdc-3820-4658-8bbe-560f106c019b. Access on: August 17, 2020.

ORTEGA, J. A.; GARZÓN HEYDT, G. Geomorphological and sedimentological analysis of flash-flood deposits: The case of the 1997 Rivillas flood (Spain). **Geomorphology**, v. 112, n. 1, p. 1–14, 2009. https://doi.org/10.1016/j.geomorph.2009.05.004

PAREDES, J. M.; OCAMPO, S. M.; FOIX, N.; OLAZÁBAL, S. X.; VALLE, M. N.; MONTES, A.; ALLARD, J. O. **Geomorphic and Sedimentological Impact of the 2017 Flash Flood Event in the City of Comodoro Rivadavia (Central Patagonia, Argentina)**. (P. Bouza, J. Rabassa, A. Bilmes, Eds.) Advances in Geomorphology and Quaternary Studies in Argentina. **Anais**...Cham: Springer International Publishing, 2021. https://doi.org/10.1007/978-3-030-66161-8_1.

PAULA, E. V. **Análise da produção de sedimentos na área de drenagem da Baía de Antonina/PR: uma abordagem geopedológica**. Thesis (Doctorade in geography) – Curitiba: UFPR. 2010.

PAULA, E. V. Análise da Produção de Sedimentos na Área de Drenagem da Baía de Antonina, Paraná: Contribuições ao planejamento do território. In: REIS, R. A. et al. (Eds.). **Litoral do Paraná: Território e Perspectivas**. Curitiba: Brazil Publishing, 2016. p. 11–35.

PAZ, O. L. S.; PAULA, E. V. Planície do Rio Jacareí após os movimentos de massa de 2011: considerações a partir da análise granulométrica de trincheira e mudanças do canal. **Revista Cerrados**, v. 19, n. 1, p. 83–99, 2021. https://doi.org/10.46551/rc24482692202106%20

PICANÇO, J. L.; NUNES, L. H. A severe convective episode triggered by accumulated precipitation in the coast of Paraná state, Brazil. 2013. In: European Conference on Severe Storms, 7. p. 3-7. Available: https://www.researchgate.net/publication/305699009_A_Severe_convective_episode_triggered_by_accumulated_precipitation_in_the_coast_of_Parana_State_Brazil Access on: May 15, 2020.

PINTO, R. C.; PASSOS, E.; CANEPARO, S. C. Classificação dos movimentos de massa ocorridos em março de 2011 na Serra da Prata, Estado do Paraná. **Geoingá: Revista do Programa de Pós-Graduação em Geografia**, v. 4, n. 1, p. 3–27, 2012. https://doi.org/10.4025/geoinga.v4i1.49152

PINTO, R. C.; PASSOS, E.; CANEPARO, S. C. Movimentos de Massa como Processos Naturais de Evolução das Encostas, Estudo de Caso: Bacia do Rio Jacareí, Municípios de Morretes e Paranaguá–PR. **Geoingá: Revista do Programa de Pós-Graduação em Geografia**, v. 6, n. 1, p. 23–45, 2014. https://doi.org/10.4025/geoinga.v6i1

REGMI, N. R.; GIARDINO, J. R.; MCDONALD, E. V; VITEK, J. D. A Review of Mass Movement Processes and Risk in the Critical Zone of Earth. In: GIARDINO, J. R.; HOUSER, C. (Eds.). **Developments in Earth Surface Processes**. Elsevier, 2015. v. 19p. 319–362. https://doi.org/10.1016/B978-0-444-63369-9.00011-2

ROSS, J. L. S.; FIERZ, M. S. M. A Serra do Mar e a Planície Costeira em São Paulo: morfogênese, morfodinâmica e as suas fragilidades. **Boletim Paulista de Geografia**, n. 100, p. 17–38, 2018. Available: https://publicacoes.agb.org.br/index.php/boletim-paulista/article/view/1497. Access on: January 26, 2022

RUTYNA, B. B.; SOARES, C. R.; WROBLEWSKI, C. A.; PAULA, E. V. Assoreamento nas baías de Antonina e de Paranaguá – PR: análise integrada das áreas fontes de sedimentação e obras de dragagem. **Revista Brasileira de Geografia Física**, v. 14, n. 2, p. 676–693, 2021. https://doi.org/10.26848/rbgf.v14.2.p676-693

SALAZAR JUNIOR, O. **Vista em sobrevoo das cicatrizes na Serra da Prata no desastre águas de março**. MINEROPAR - Minerais do Paraná. 2011a. 1 fotografia, color.

SALAZAR JUNIOR, O. **Vista em sobrevoo da ponte destruída da BR 277 sobre o rio Jacareí.** MINEROPAR - Minerais do Paraná. 2011b. 1 fotografia, color.

SANTOS, R. D.; LEMOS, R. C.; SANTOS, H. G.; KER, J. C.; ANJOS, L. H. C.; SHIMIZU, S. H. **Manual de descrição e coleta de solo no campo**. Viçosa: Sociedade Brasileira de Ciência do Solo, 2015.

Secretaria Municipal de Meio Ambiente de Paranaguá (SEMMA). **Imagem pancromática WorldView-1**. Litoral do Paraná, 2019. Imagem de satélite. WorldView-1, 2 mai 2011.

SILVEIRA, C. T.; FIORI, A. P.; SCHILIPACK, P.; DIAS, S. M. Mapeamento preliminar da suscetibilidade natural a movimentos de massa da Serra do Mar Paranaense apoiado na análise digital do relevo. **Revista Brasileira de Geomorfologia**, v. 15, n. 1, 2014. http://dx.doi.org/10.20502/rbg.v15i1.366

SILVEIRA, C. T. DA; FIORI, A. P.; FERREIRA, A. M.; GÓIS, J. R. DE; MIO, G. DE; SILVEIRA, R. M. P.; MASSULINI, N. E. B.; LEONARDI, T. M. H. Emprego de atributos topográficos no mapeamento da susceptibilidade a processos geoambientais na bacia do rio Jacareí, Paraná. **Sociedade & Natureza**, 2013. https://doi.org/10.1590/S1982-45132013000300014

STEVAUX, J. C.; LATRUBESSE, E. M. **Geomorfologia fluvial**. 1. ed. São Paulo: Oficina de Textos, 2017.

TEIXEIRA, M. S.; SATYAMURTY, P. Trends in the Frequency of Intense Precipitation Events in Southern and Southeastern Brazil during 1960–2004. **Journal of Climate**, v. 24, n. 7, p. 1913–1921, 2011. https://doi.org/10.1175/2011JCLI3511.1

VIEIRA, B. C.; GRAMANI, M. F. Serra do Mar: the most “tormented” relief in Brazil. In: **Landscapes and landforms of Brazil**. Springer, 2015. p. 285–297. https://doi.org/10.1007/978-94-017-8023-0_26

WANG, B.; LI, Y.; LIU, D.; LIU, J. Debris flow density determined by grain composition. **Landslides**, v. 15, n. 6, p. 1205–1213, 2018. https://doi.org/10.1007/s10346-017-0912-x

YANG, T.; LI, Y.; ZHANG, Q.; JIANG, Y. Calculating debris flow density based on grain-size distribution. **Landslides**, v. 16, n. 3, p. 515–522, 2019. https://doi.org/10.1007/s10346-018-01130-2

ZAPATA, R.; SIMIANO, L. F.; PINHEIRO, E. G. O EVENTO ÁGUAS DE MARÇO E SUA AVALIAÇÃO DE DANOS E PERDAS. In: PINHEIRO, E. G.; PEDROSO, F. F. F. (Eds.). **CONSTRUINDO UM ESTADO RESILIENTE: O MODELO PARANAENSE PARA A GESTÃO DO RISCO DE DESASTRES**. 1. ed. Curitiba: CEPED/FUNESPAR, 2016. p. 34–51.

ZERI, M.; S. ALVALÁ, R.C.; CARNEIRO, R.; CUNHA-ZERI, G.; COSTA, J.M.; ROSSATO SPATAFORA, L.; URBANO, D.; VALL-LLOSSERA, M.; MARENGO, J. Tools for Communicating Agricultural Drought over the Brazilian Semiarid Using the Soil Moisture Index. **Water,** v. 10. p. 1-15, 2018. https://doi.org/10.3390/w10101421

AUTHORS' CONTRIBUTION

Otacílio Lopes de Souza da Paz conceived the study, developed the proposed methodology, collected and analyzed the data and wrote the text. Eduardo Vedor de Paula conceived the study and contributed to the text. He conducted field campaigns and discussed the results obtained. Responsible for the acquisition of financing. Coordinator of the laboratory where this research was developed.